Role of magnetic 'structure' in determining in vivo relaxivity-iron behavior: Size does matter.

N. R. Ghugre[1,2], and J. C. Wood[1,2]

[1]Division of Cardiology, Childrens Hospital Los Angeles, Keck School of Medicine, University of Southern California, Los Angeles, CA, United States, [2]Department of Radiology, Childrens Hospital Los Angeles, Keck School of Medicine, University of Southern California, Los Angeles, CA, United States

Introduction: Iron overload is a serious condition for patients with thalassemia major, transfusion-dependent sickle cell anemia and inherited disorders of iron metabolism (1). MRI is becoming increasingly important in non-invasive quantification of tissue iron, overcoming the drawbacks of traditional techniques. Super-paramagnetic tissue iron deposits produce magnetic field disturbances that increase MRI relaxivities R2 (1/T2) and R2* (1/T2*). R2* rises linearly with iron while R2 has a curvilinear relationship. Although the two recent independent studies by St. Pierre et. al. (2) and Wood et. al. (3) have demonstrated reproducible R2 and R2* calibrations, tissue iron quantitation has unresolved clinically-relevant problems. Recalibration remains a concern for changes in 1) MRI sequences and parameters, 2) tissue in question and 3) iron removal chelation therapy; knowledge of underlying biophysics will help resolve these issues. Moreover, it will allow understanding of incompletely explained phenomena, such as the nonlinearity of the R2-iron curve and the relevant iron "scales" imaged by R2 and R2* methods. Toward this end, we employed a Monte Carlo model-based approach using human liver as a 'model' tissue system to determine the contribution of iron particle size and distribution on MRI signal relaxation. A validated and optimized model will aid understanding and quantitation of iron-mediated relaxivity in tissues where biopsy is not feasible (heart, pancreas).

Methods: An iron concentration (FE) range of 0.5-30 mg/g dry tissue was chosen for simulation purpose, representing the most relevant fraction of the pathologic range. The iron deposits were modeled as homogeneous spheres with susceptibility as a 4:1 mixture of hemosiderin and ferritin using literature values (4) of $9.4E^{-8}$ and $11.1E^{-8}$ (mg FE/g)$^{-1}$ cgs units. Diffusion of water molecules (diffusion constant, D= 0.76 μm^2/ms for human liver) was freely isotropic in three dimensions but constrained not to pass into the spheres. For given FE, size distribution of spheres was approximated using low order Gamma function fitted to lysosomal-histograms obtained from electron micrographs of human liver biopsy specimens (5). Volume fraction of spheres in tissue (0.67-4.04%) was quadratic with FE. A cuboidal tissue environment (40 μm side) mimicking human liver was simulated consisting of 64 hepatocytes (cells) approximated by 10 μm side cubes (Fig. 1). Within this milieu, spheres were distributed in two fashions: 1) uniform distribution and 2) a Gaussian probability distribution function having a coefficient of variation of 12.5%. For each distribution, protons were either 1) allowed to pass through the cell wall (unrestricted diffusion) or 2) not (restricted). Hence, in the total of four cases (uniform-restricted, uniform-unrestricted, Gaussian-restricted, Gaussian-unrestricted), the magnetic field experienced by the protons was computed as a superposition of magnetic dipoles. Using phase accrual of proton population, the field induction decay was then measured along with a single echo experiment to obtain relaxivities R2* (1/T2*) and R2 (1/T2). The model neglected any sort of contact or exchange mechanisms. The results were compared with published *in vivo* calibrations.

Figure 1

Results: For a given type of sphere distribution, R2 and R2* remained comparable whether protons experienced restricted or unrestricted diffusion. In contrast, varying the average cellular iron concentration (Gaussian distribution) reduced R2* by 20% and R2 by 50% compared to uniformly distributed iron. Fig. 2 demonstrates predicted R2* against FE, using a 'Gaussian-restricted' model, overlaid on the *in vivo* calibration curve derived by Wood et. al. (3). The model accurately predicted both the mean and the standard deviation of the R2* calibration curve. Fig. 3 shows predicted R2 as a function of FE along with calibration curve derived by St. Pierre et. al. (2). The predicted R2 points divide the calibration curve into two distinct regimes with a breakpoint of 12.5 mg/g. R2-iron predictions agree closely with the curvilinear R2 calibration below the breakpoint, but they systematically overestimate true iron levels beyond it.

Figure 2

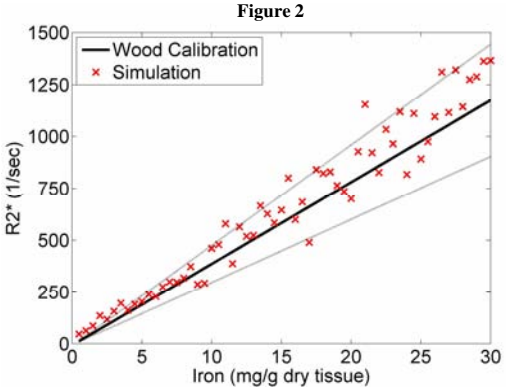

Figure 3

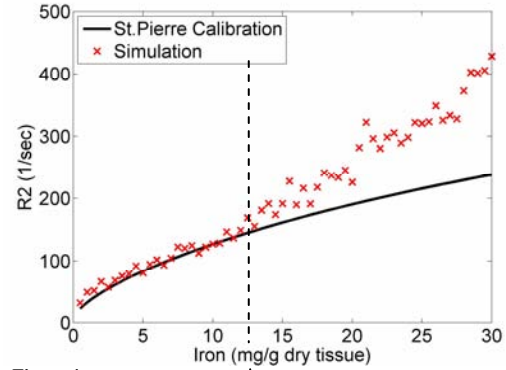

Discussion: Tissue iron is primarily stored as ferritin-clusters or insoluble hemosiderin deposits in cytoplasmic saccules known as lysosomes. Previous *in vitro* work has demonstrated that iron aggregation greatly amplifies local diffusion gradients, increasing transverse relaxivity six-fold compared with ferritin in solution or gel (6). Relative proton inaccessibility to lysosomal-iron further reduces the contribution of dipole-dipole interactions (7). In fact, we are able to accurately model both R2 and R2* iron calibrations up to 12.5 mg/g simply by modeling susceptibility based diffusion losses (no contact relaxivity mechanisms). The model even captured the strong curvilinearity at low iron concentrations (near the normal level of 1 mg/g). The systematic R2 overestimation at high iron concentration is predictable by examination of tissue histology. Fig. 4 shows light micrographs of representative human liver samples where FE is indicated by the blue stain. It is clear that with progressive increase of FE, larger secondary iron structures (5-15 μm) become predominant in the reticulo-endotheliel spaces of the liver (arrows in Fig. 4); these were neglected in our model. Iron deposits greater than 0.8 μm radius experience static refocusing, yielding lower R2 values for a given amount of tissue iron (8). Hence for complete R2-FE calibration, it is essential to characterize both intra- and inter-hepatocyte iron pools. R2* measurements, lacking static refocusing, maintain linearity over the clinical range of iron deposition; this behavior was captured by our model.

With novel chelation therapies for iron removal, R2 calibration curve may be systematically altered depending on the chelators response to each iron pool; modeling will be able to account for redistributed iron. Furthermore, a validated and optimized tissue-specific model will be capable of providing iron concentration estimates for inaccessible organs (heart, brain, pancreas) where tissue biopsy is not an option for calibration purposes.

Figure 4

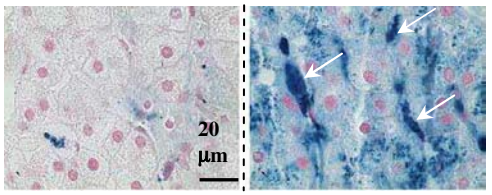

FE = 1.4 mg/g **FE = 30 mg/g**

Acknowledgements: GCRC (RR00043-43), NIH (1 R01 HL75592-01A1), Saban Research Institute (CHLA), The Wright Foundation.

References: 1) Gordeuk VR et. al., Annu Rev Nutr 1987;7:485-508.
2) St Pierre TG, Clark PR, Chua-anusorn W, et al., Blood 2005; 105:855-861.
3) Wood JC, Enriquez C, Ghugre N, et al., Blood 2005; 106:1460-1465.
4) Michaelis J, Coryell C, Granick S., J Biol Chem 1943; 148:463-380.
5) Ghugre N, Coates TD, Nelson MD, Wood JC, Mag Res Med 2005; 54:1185-1193
6) Wood JC, Fassler J, Meade T., Mag Res Med 2004;51:607-611.
7) Gossuin Y, Muller RN, Gillis P., NMR Biomed 2004; 17:427-432.
8) Ghugre N, Wood JC, Proc. Intl. Soc. Mag. Reson. Med 14, 2006; 2522.